Effect of Implant Diameter and Ridge Dimension on Stress Distribution in Mandibular First Molar Sites—A Photoelastic Study

Deborah Termeie, DDS[1]*
Perry R. Klokkevold, DDS, MS[2]
Angelo A. Caputo, PhD[3]

The long-term clinical success of a dental implant is dependent upon maintaining sufficient osseointegration to resist forces of occlusion. The purpose of this study was to investigate the effect of implant diameter on stress distribution around screw-type dental implants in mandibular first molar sites using photoelastic models. The design included models with different buccal-lingual dimension. Twelve composite photoelastic models were assembled using 2 different resins to simulate trabecular and cortical bone. Half of the models were fabricated with average dimensions for ridge width and the other half with narrower buccal-lingual dimensions. One internal connection implant (13 mm length) with either a standard (4 mm), wide (5 mm), or narrow (3.3 mm) diameter was embedded in the first molar position of each photoelastic model. Half the implants were tapered and the other half were straight. Full gold crowns in the shape of a mandibular first molar were fabricated and attached to the implants. Vertical and angled loads of 15 and 30 pounds were applied to specific points on the crown. Wide-diameter implants produced the least stress in all ridges while narrow-diameter implants generated the highest stress, especially in narrow ridges. It may be that the volume and quality of bone surrounding implants influences stress distribution with a greater ratio of cortical to trabecular bone, thus providing better support. Models with wide-diameter implants loaded axially had a more symmetrical stress distribution compared to standard and narrow diameter implants. A more asymmetrical stress pattern developed along the entire implant length with angled loads. Implant diameter and ridge width had considerable influence on stress distribution. Narrow-diameter implants produced more stress than wide diameter implants in all conditions tested.

Key Words: dental implants, photoelastic models, stress distribution, bone configuration

INTRODUCTION

The long-term clinical success of a dental implant is dependent upon acquiring and maintaining sufficient bone support with osseointegration to resist forces of occlusion without excessive bone loss. A critical factor in establishing and maintaining osseointegration is native bone, which is typically comprised of an outer layer of cortical bone and an inner layer of marrow and cancellous bone. According to the established criteria[1] for the assessment of implant survival and success, marginal bone level change in the first year should be less than 1.5 mm, and ongoing annual bone loss should be less than 0.2 mm.[2] Bone support and resistance play important roles in the long-term success of the implant retained/supported prosthesis.

The greatest stress occurs at the abutment-implant interface.[3] A recent study[4] found when the implant diameter is increased, stress values and concentration areas decrease for cortical bone. The study also found increased implant length improved stress distributions for cancellous bone.

Wide-diameter implants can be used advantageously to immediately replace failed implants. The increased diameter occupies a larger space and allows better stability. One study found that over a two-year period, 196 patients with 268 wide-diameter implants had an overall success rate of approximately 96%.[5] Another study[6] found 5 mm–wide-diameter implants to be more favorable with regard to distribution of stresses compared to standard diameter implants (3.75 mm). Standard diameter implants had the largest areas and the most intense stress. The study also found that a lateral load caused the highest stresses. Hence, wide-diameter implants reduce stress in the bone surrounding the implant, and also dissipate the forces. In sites limited by the ridge height, the use of wide implants with shorter length may be a viable alternative.[7]

Initial opposition towards wide-diameter implants stemmed from studies reporting higher failure rates that focused mostly on the likelihood that wider drills generated excessive heat during preparation of the osteotomy site. One study found that the greatest temperature increase was observed with the 2 mm twist drill at both 4 and 8 mm depths.[8] A significantly greater temperature increase was noted at the 8 mm depth compared to the 4 mm depth with twist

[1] Periodontics, UCLA School of Dentistry, Los Angeles, Calif.
[2] Postgraduate Periodontics, UCLA School of Dentistry, Los Angeles, Calif.
[3] Deceased; previously with Advanced Prosthodontics, Biomaterials, and Hospital Dentistry, UCLA School of Dentistry, Los Angeles, Calif.
* *Corresponding author,* e-mail: dtermeie@ucla.edu
DOI: 10.1563/aaid-joi-D-14-00008

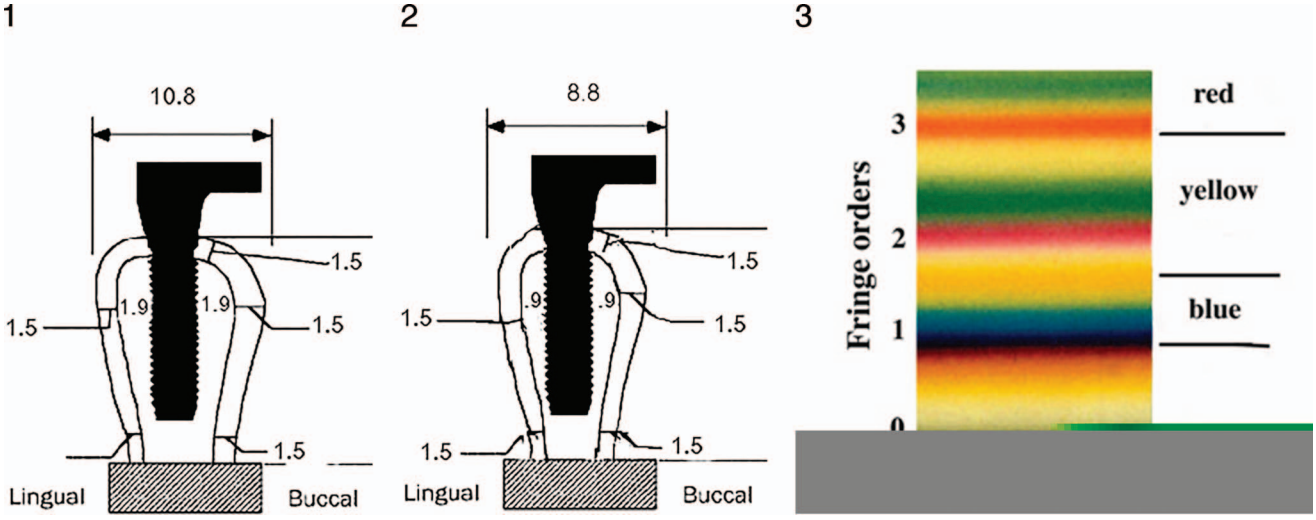

Figures 1–3. Figure 1. Diagram of average ridge with a standard-diameter (4 mm) implant showing dimensions of cortical and trabecular bone surrounding the implant. **Figure 2.** Diagram of narrow ridge with a standard-diameter (4 mm) implant showing dimensions of cortical and trabecular bone surrounding the implant. **Figure 3.** Interpretation of the fringe order.

drills. This contradicts the argument that wide-diameter drills were responsible for overheating the bone. In fact, the higher failure rates of wide-diameter implants may have been due to their use in rescue procedures at failed implant sites or because they were placed in areas with inadequate bone width.

The purpose of this study was to investigate the effect of implant diameter on stress distribution within the supporting structure around narrow-, standard-, and wide-diameter screw-type implants with straight and tapered designs. To further evaluate the effect of implant diameter on stress distribution, photoelastic models with average vs narrow buccal-lingual dimensions were tested with each implant.

Materials and Methods

Photoelastic model

Twelve composite photoelastic models were assembled using 2 different resins to simulate the anatomy of trabecular and cortical bone for quasi–three-dimensional photoelastic analysis. The photoelastic materials were selected to reproduce a reasonable ratio of the elastic modulus between cortical and trabecular bone. Half of the models were fabricated with average buccal-lingual dimensions (B-L) for the ridge, and the other half of the models were fabricated with a narrower buccal-lingual dimension (Figures 1 and 2, Tables 1 through 3). Studies have shown that the cortical thickness in the mandibular edentulous site is about 2 mm on the buccal and 2 mm on the lingual. Our model has 1.5 mm cortical bone width on the buccal and 1.5 mm on the lingual.[9] Half-arch mandibular models were fabricated without teeth. The models spanned from the second molar to the canine region.

The master model of cortical bone and trabecular bone were made with high-strength dental stone (Hard Rock, Whip Mix, Louisville, Ky). An impression of the complex was taken using silicone impression material (3110 RTV, Dow Corning, Midland, Mich), which served as a master mold for the photoelastic cortical and trabecular bone model. Dental stone was poured into the silicone impression. Burs with stops were used to remove a uniform 1.5 mm outer layer of stone (cortical bone dimensions) from the buccal, lingual, and crest of the ridge. Another silicone impression was made of the remaining stone model, which represented the dimension of the trabecular bone. A photoelastic resin (PLM-2, Photolastic Division, Measurements Group, Raleigh, NC) was injected into the silicone impression. Upon completion of polymerization, the trabecular resin model was placed into the master silicone mold, and photoelastic resin (PLM-1, Measurements Group) was injected to surround and attach to the trabecular resin model. Channels were made in the master mold silicone impression to allow for PLM-1 to attach to the trabecular bone model and to prevent bubble formation. The inferior surface of the trabecular bone was roughened with abrasive papers to enhance micromechanical retention of the second resin material (cortical bone).

Implants

All test implants were 13 mm length internal connection (Lifecore Biomedical, Chaska, Minn). Four implants were standard (4 mm) diameter, four implants were wide diameter (5 mm), and four implants were narrow (3.3 mm) diameter. One standard-diameter implant (4 × 13 mm) was embedded in each of 4 photoelastic models. A wide diameter (5 × 13 mm) implant was embedded in 4 other models, and lastly, to fully appreciate the range of implant diameter effects, a narrow diameter (3.3 × 13 mm) implant was embedded in 4 other models (Table 4). The implants were completely embedded in resin, representing complete integration. Both tapered and straight implant designs were used for each implant size to evaluate the effect of shape on stress distribution.

Crowns representing mandibular first molars were waxed, invested, and cast with metal (70% palladium, Argen, San Diego, Calif). All crowns were nearly identical in shape and dimension, except the implant-abutment connection dimen-

Table 1

Model dimensions and implants used in the study*

	Average Arch B-L Width 10.8 mm	Narrow Arch B-L Width 8.8 mm
Implant size placed (mm)	Wide diameter 5 × 13 Standard diameter 4 × 13 Narrow diameter 3.3 × 13	Wide diameter 5 × 13 Standard diameter 4 × 13 Narrow diameter 3.3 × 13

*B-L indicates bucco-lingual.

sion was made to fit flush with the implant diameter. The crowns were made with flat occlusal contacts and rounded marginal ridges to facilitate consistent application of the load cell tip and prevent deflection when loads were applied. Loads were placed on the mesiobuccal and distobuccal cusps of the crown.

Axial and nonaxial (20 degrees to implant axis) loads of 15 and 30 pounds were applied with a calibrated load cell (100 pound low-range transducing cell, GM2 Universal Transducing Cells, Camarillo, Calif) to the mesiobuccal and distobuccal of each crown. Loads were monitored using a strain gauge conditioner (Measurements Group). The load level was selected because it is close to the actual functional load levels[10] and provides an optimal response in photoelastic materials without permanent damage. The first molar was selected for loading in this study because maximum occlusal forces are often exerted in this region where there is maximum contraction of the elevator muscles.[11] The mesiobuccal and distobuccal cusps were selected because they typically incur the most force in the mouth. The models were immersed in mineral oil to minimize surface refraction and facilitate photoelastic observation. The temperature of the oil was maintained between 76°F and 78°F. The stresses that developed in the photoelastic models were visualized and recorded photographically with a digital camera in the field of a circular polariscope, and the results were analyzed.

Determination of stress intensity was accomplished by counting the fringe number (Figure 3), which is proportional to maximum shear strength. Fringe numbers were determined at: (1) the crest of the bone model around the implant neck, (2) below the interface of the two materials along the implant body, and (3) around the apex of the implant. Fringe numbers were counted on both sides (mesial and distal) of the implant for axial and angled loads. Observations of fringe order numbers resulting from various loading conditions were made on the digital photographs, which were subsequently viewed with a computer graphics program (Photoshop 4.0 Adobe Systems, San Jose, Calif). A fringe number count of 3 or greater was considered higher stress, and a fringe number count below 2 was considered lower stress. Two investigators (D.T. and A.C.) counted fringe numbers and evaluated stress distribution patterns for all models independently. The results were reported by consensus.

Results

Prior to application of loads, each model was examined in the circular polariscope to check for inherent stress. Since only very low stresses (fringe number <1) were noted, the stress patterns that developed under load could be attributed to the applied load.

The results of the 15-pound loads were proportional to the 30-pound loads. For simplicity, the data obtained with 30-pound loads are presented.

For both tapered and straight implants, when an axial load was applied to the center of the implant, the highest stress concentration was located within the crestal cortical layer, and the stresses were distributed symmetrically around the implant. No significant differences were observed when comparing

Table 2

Dimensions of bone in the narrow ridge model

Implant Diameter (mm)	Total Width (mm)	Width of Cortical Bone (mm)	Width of Trabecular Bone (mm)	Width of Trabecular Bone Surrounding Implant (mm)
3.3	8.8	3	5.8	2.5
4	8.8	3	5.8	1.8
5	8.8	3	5.8	0.8

Table 3

Dimensions of bone in the average ridge model

Implant Diameter (mm)	Total Width (mm)	Width of Cortical Bone (mm)	Width of Trabecular Bone (mm)	Width of Trabecular Bone Surrounding Implant (mm)
3.3	10.8	3	7.8	4.5
4	10.8	3	7.8	3.8
5	10.8	3	7.8	2.8

TABLE 4

Model descriptions*

Model	Ridge Width (mm)	Implant Diameter (mm)
NR-WD	8.8	5
AR-WD	10.8	5
NR-SD	8.8	4
AR-SD	10.8	4
NR-ND	8.8	3
AR-ND	10.8	3

*NR indicates narrow ridge; WD, wide diameter; AR, average ridge; SD, standard diameter; ND, narrow diameter.

tapered and straight implants of similar diameter. Thus, only photoelastic images of tapered implants are included in this paper.

Wide-diameter implants in the narrow ridge were associated with higher stress to the model than wide-diameter implants in the average ridge. Narrow-diameter implants were associated with higher stress when placed in narrow ridges compared to wide-diameter implants placed in narrow ridges.

Tapered implants

Implants were axially loaded with a 30-pound load in the center of the crown. The results showed that NR-ND (narrow ridge with a narrow-diameter implant) had greater stress than NR-WD (narrow ridge with a wide-diameter implant) or AR-WD (average ridge with a wide-diameter implant) at the crest and at the interface of the cortical and trabecular bone. Although there is greater trabecular bone in AR-ND (average ridge with a narrow-diameter implant), it still showed more stress than AR-WD. Because NR-ND and AR-ND showed close isochromatic fringes at the interface and crest, they both demonstrated greater stress concentration compared to the other models.

Similarly, when a 30-pound load was placed axially on the mesiobuccal cusp of the crown (Table 5 and Figure 4), NR-ND demonstrated greater stress at the crest of the model than NR-WD. All models showed higher stress on the mesial of the implant when mesial loads were applied. In an overall comparison of all configurations, the AR-WD had the least stress at the crest and apex. It was also found that AR-WD had less stress than NR-WD.

A 30-pound load was also placed axially on the distobuccal cusp of the crown. Again, NR-ND had higher stress than NR-WD and AR-WD at the interface and at the crest. As expected, the distal of all the models showed more stress than other areas when distal loads were applied. In this case, the average diameter implants had the most stress. The apex on all models showed similar stress with the exception of NR-WD, which showed the least amount of stress at the apex.

Thirty-pound nonaxial loads were also placed on the models. The first load situation was on the mesiobuccal cusp (Table 6 and Figure 5). The results with angled loads were similar to those with axial loads; however, the stress had a greater mesial distribution. Since NR-ND and AR-ND showed close isochromatic fringes at the interface and crest, they both demonstrated high stress concentration. NR-WD had greater stress than AR-WD on the mesial of the implant, but AR-WD and NR-WD had similar stress on the distal. In comparison of all model configurations, NR-SD and NR-ND had the most stress. In contrast to the axial load, a more asymmetrical distribution developed with angled loads.

When a 30-pound nonaxial load was placed on the distobuccal cusp, NR-WD had the most uniform distribution in the model. In the narrow ridge configurations, NR-ND had the highest stress; however, in the average ridges, AR-SD had the highest stress generated in the model on the distal and AR-ND had the greatest stress on the mesial. The apices of all the models showed similar stress patterns. Furthermore, NR-WD, which has minimal trabecular bone surrounding the implant, was found to have more stress in the model compared to AR-WD. Applying the load at a 20-degree angle accentuated the findings with an axial load on the distobuccal cusp.

Straight implants

Similar to the tapered implants, models were loaded axially with a 30-pound load at the center of the crown. AR-ND had the highest stress on the mesial of the model. In a comparison of the narrow ridge models, the narrow-diameter implant (NR-ND) had the highest stress to the model. Likewise, in a comparison of the average ridge models, the narrow-diameter implant (AR-ND) had the highest stress. Most of the stress was on the mesial of the model. Apices of the models had similar stress values.

A 30-pound axial load was also placed on the mesiobuccal cusp of the model (Table 7). It was found that AR-ND had the highest stress, with the greatest stress found on the mesial of all the models. NR-SD and NR-WD had similar stress at the crest and interface. NR-ND had higher stress than NR-WD and AR-WD; NR-WD had greater stress than AR-WD. In a comparison of the narrow ridge configurations, NR-ND had the highest stress. Overall, AR-WD had the lowest stress, and the stress was

TABLE 5

Stress distribution (fringe numbers) for tapered implants with 30-lb axial load applied to the mesiobuccal cusp of the crown

Implant Diameter	Ridge Dimension	Stress at Crest	Stress Pattern at Interface	Stress Pattern at Apex	Sum
Wide	Narrow	3	2+	1+	6++
Wide	Average	2	2+	1+	5++
Standard	Narrow	3	3	2	8
Standard	Average	3+	2+	2	7++
Narrow	Narrow	3+	1+	3	7++
Narrow	Average	2	3	2	7

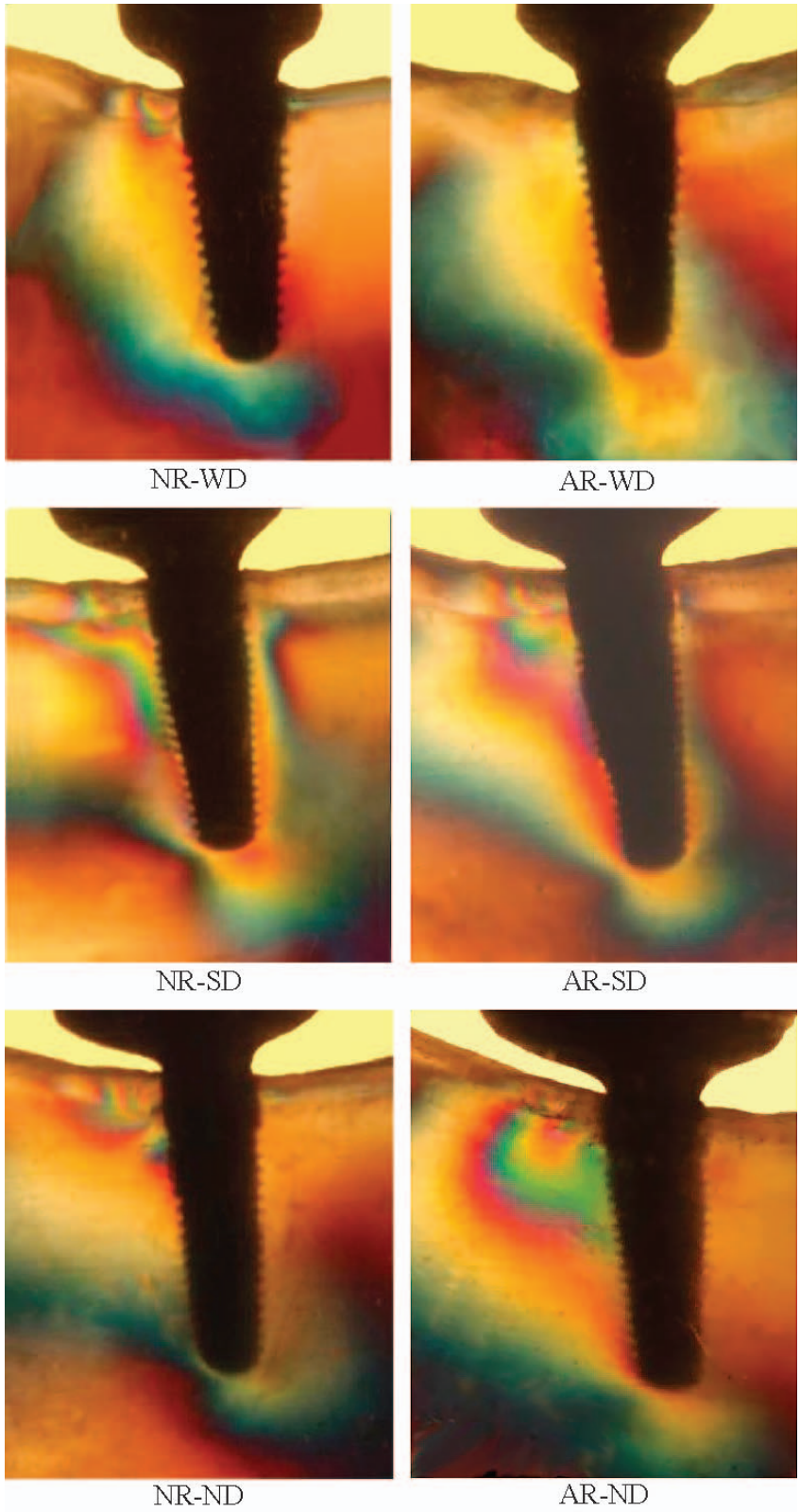

Figure 4. MB axial load (tapered): NR-WD (5 mm-diameter implant in a narrow ridge), AR-WD (5 mm-diameter implant in an average ridge), NR-SD (4 mm-diameter implant in a narrow ridge), AR-SD (4 mm-diameter implant in an average ridge), NR-ND (3.3 mm-diameter implant in a narrow ridge), and AR-ND (3.3 mm-diameter implant in an average ridge).

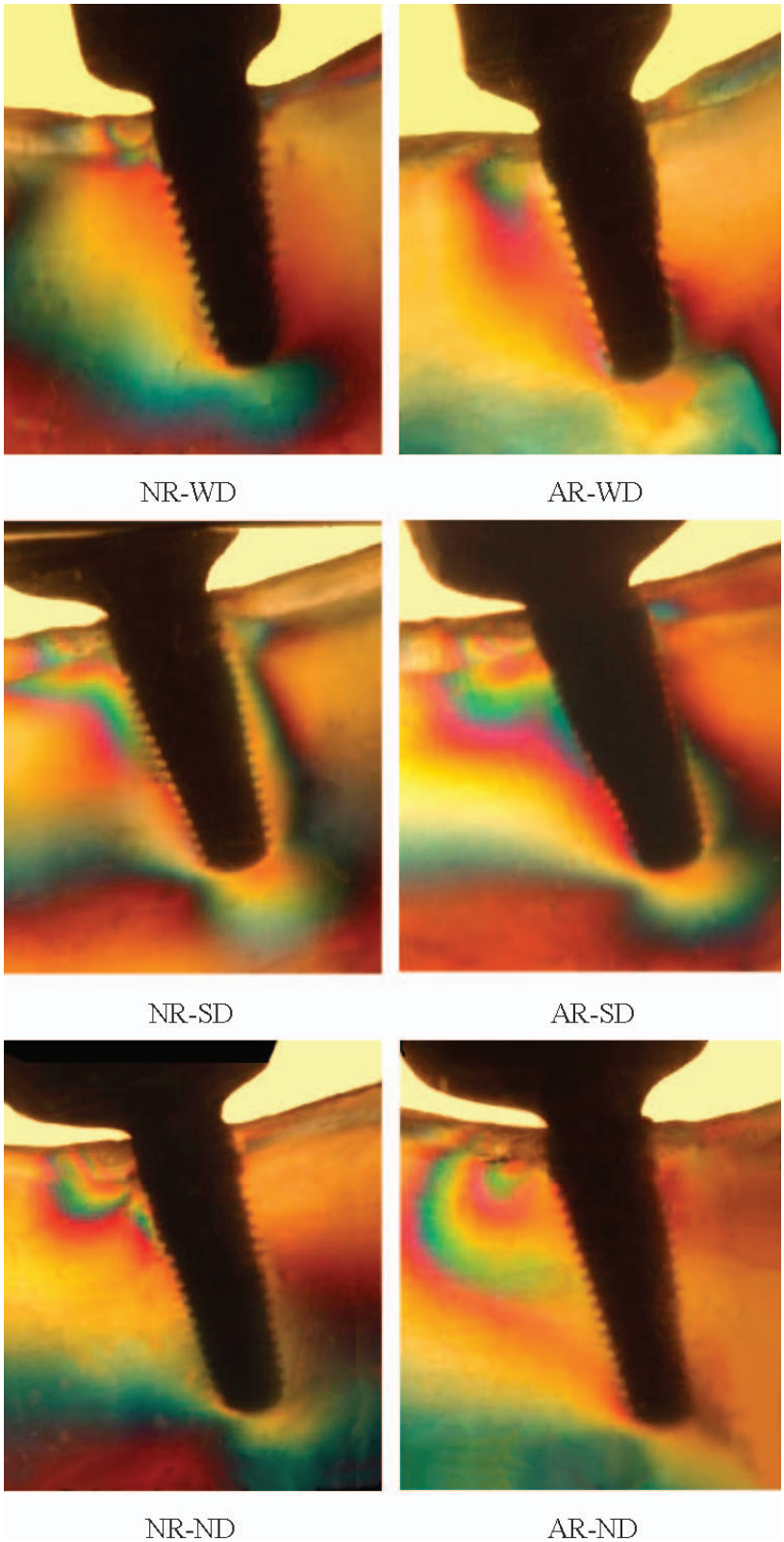

Figure 5. MB nonaxial load (tapered): NR-ND (5 mm-diameter implant in a narrow ridge), AR-WD (5 mm-diameter implant in an average ridge), NR-SD (4 mm-diameter implant in a narrow ridge), AR-SD (4 mm-diameter implant in an average ridge), NR-ND (3.3 mm-diameter implant in a narrow ridge), and AR-ND (3.3 mm-diameter implant in an average ridge).

Table 6

Stress distribution (fringe numbers) for tapered implants with 30-lb nonaxial load applied to the mesiobuccal cusp of the crown

Implant Diameter	Ridge Dimension	Stress at Crest	Stress Pattern at Interface	Stress Pattern at Apex	Sum
Wide diameter	Narrow	3+	2+	1+	6+++
Wide diameter	Average	2+	1+	2+	5+++
Standard diameter	Narrow	3+	3+	2	8++
Standard diameter	Average	3+	3	2	8+
Narrow diameter	Narrow	4	3+	1+	8++
Narrow diameter	Average	3+	3	2	8+

distributed uniformly in the model. Apices of the models had similar stress values.

The 30-pound axial loads were also placed on the distobuccal cusp of the crown. Analyzing all the straight implant models showed that AR-WD had the least stress while NR-ND had the highest stress, especially on the distal cusp of the crown. Because NR-ND showed close isochromatic fringes at the interface and crest, it also demonstrated higher stress compared to the other models. In a comparison of all the narrow ridges, NR-WD (narrow ridge with a wide-diameter implant) had the least stress, and NR-ND had the greatest stress. In a comparison of all the average ridges, AR-ND (average size ridge with a narrow-diameter implant) had the most stress while AR-WD had the least stress. Apices for all the models had similar stress values, and the most stress was found on the distal of the models.

When 30-pound angled loads were placed on the mesiobuccal cusp (Table 8), the models showed increased stress compared to the nonangled models. AR-WD continued to have the least stress. In the narrow ridges, NR-ND had the highest stress. Because NR-ND showed close isochromatic fringes at the mesial interface and crest, it demonstrated greater stress concentration compared to the other model configurations. Comparing the average ridges, AR-WD (2.8 mm trabecular bone) had the least stress and AR-ND (4.5 mm trabecular bone) had the greatest stress. At the interface of trabecular and cortical bone, NR-ND and AR-ND had the highest stress, while AR-WD had the least.

Angled loads of 30 pounds placed on the distobuccal cusp showed that AR-WD had the lowest stress and AR-ND had the highest stress. In comparison of the narrow ridges, NR-ND had the highest stress and NR-WD had the least stress generated in the model. In a comparison of the average ridges, AR-ND had the highest stress and AR-WD had the least stress. As opposed to nonaxial loads on the mesiobuccal cusp, the load on the distobuccal cusp produced similar stress at the interface.

Discussion

The photoelastic model configuration employed in this study represented the right posterior segment of an edentulous mandible. Two different photoelastic resins were used to anatomically simulate the qualities of cortical and trabecular bone. The proportion of cortical and trabecular bone was based on studies conducted by Katranji et al[9] and Deguchi et al.[12] The ratio of elastic moduli between cortical and trabecular bone stimulants (PLM-1 and PLM-2, respectively) falls into a realistic range.[13] These models facilitate explanation of perplexing bone conditions. Stress studies have shown that photoelastic analysis and finite element studies compare favorably.[14]

The results of this study show that narrow-diameter implants were associated with more stress when placed in narrow ridges, and wide-diameter implants had the least stress in both average and narrow ridges. The results also showed that models with a wide-diameter implant had a more symmetrical stress distribution pattern when compared to the average- and narrow-diameter implants. These findings suggest that wide-diameter implants tolerate occlusal forces better than average- and narrow-diameter implants in the posterior mandible, which is consistent with previous studies. Graves et al placed 268 wide-diameter (5 and 6 mm) implants over a 2-year period.[15] Their overall success rate was approximately 96%. Albiol et al found that 20 of the 21 fractured implants (from 1500) evaluated in their study were 3.75 mm diameter, and the only other fractured implant was 4 mm.[16] Clearly, it has been shown that an increase in diameter increases resistance to fracture.

It may be that the volume and quality of bone surrounding implants influences stress distribution with a greater ratio of

Table 7

Stress distribution for straight implants with 30-lb axial load applied to the mesiobuccal cusp of the crown

Implant Diameter	Ridge Dimension	Stress at Crest	Stress Pattern at Interface	Stress Pattern at Apex	Sum
Wide diameter	Narrow	2	3	1+	6+
Wide diameter	Average	2+	<2	1+	5++
Standard diameter	Narrow	2	3	2	7
Standard diameter	Average	3	2+	<2	7+
Narrow diameter	Narrow	3	2+	<2	7+
Narrow diameter	Average	4	3	1+	8+

Table 8

Stress distribution for straight implants with 30-lb nonaxial load applied to the mesiobuccal cusp of the crown

Implant Diameter	Ridge Dimension	Stress at Crest	Stress Pattern at Interface	Stress Pattern at Apex	Sum
Wide diameter	Narrow	3+	3	1+	7++
Wide diameter	Average	3	2	1+	6+
Standard diameter	Narrow	3+	3	1+	7++
Standard diameter	Average	4	2+	<2	8+
Narrow diameter	Narrow	4	4	2	10
Narrow diameter	Average	4	4	2+	10+

cortical to trabecular bone providing better support. For example, this study found that a narrow-diameter implant in a narrow ridge having 2.5 mm of peri-implant trabecular bone resulted in higher stress to bone than did a wide-diameter implant in the same ridge. The wide-diameter implant had only 0.8 mm of peri-implant trabecular bone (ie, greater cortical to trabecular bone volume), suggesting that cortical bone provides better support than trabecular bone. A recent 3-D finite element analysis study[17] on stress in bone tissue around single implants with different diameters found the trabecular bone presented higher tensile stress with reduced implant diameter, consistent with the findings in this study. Models with a narrow ridge and narrow-diameter implant and models with an average ridge with a narrow-diameter implant had similar stresses at the interface because the small diameter was surrounded by greater volumes of trabecular bone. There may be a critical amount of trabecular bone that tolerates stresses well when it is surrounded and supported by cortical bone.

Clinical studies in monkeys[18] and humans[19] suggest that occlusal overload can be the main factor for the failure of an osseointegrated implant. Treatment planning should include prosthodontic considerations to reduce load-induced stresses when poor osseointegration is anticipated. Since the results of the present study demonstrated that a nonaxially directed load produced more localized and severe stresses compared to an axial load, reducing the lateral component of occlusal force by eliminating excursive interferences and reducing the occlusal table is recommended.

This study demonstrates that the wider the implant in a ridge (narrow ridge here was 8.8 mm), the less stress is generated. Model NR-WD (narrow ridge with wide-diameter implant) had 0.4 mm of buccal and lingual trabecular bone on either side of the implant, and it still had less stress when compared to a narrow-diameter implant with more trabecular bone on the buccal and lingual of the ridge (1.25 mm). Some studies have found that narrow implants have statistically lower stability values than wide implants,[20] while other studies find no association between implant diameter and early loss of implants.[21]

Tapered implants have been used because they require less space in the apical region, which is useful when roots are too close. A recent study by Kim et al[22] found that hybrid textured tapered implants placed in the posterior maxilla and mandible are predictable (with primary stability) for immediate loading. In the current study, straight implants had slightly higher stress.

A recent study found greater stress concentration in the cervical and apical thirds with axial loads.[23] However, models with an oblique load were observed to have a higher number of isochromatic fringes in the implant apex and in the cervical area adjacent to the load direction. Consistent with the findings in this study, the authors determined that an oblique load produced the highest stress in the models examined. Similarly, in this study, the straight narrow-diameter implant in an average ridge with an oblique load was found to have slightly more stress at the apex compared to the model with an axial load.

The photoelastic modeling system used in this study has limitations when predicting the response of biologic systems to applied loads. However, when under carefully controlled conditions, all of these systems can indicate where potential stress-related difficulties may arise. The results of the photoelastic information obtained in the present investigation can help the clinician by providing data on different implant diameters in different ridge configurations. As always, this information should be used in conjunction with sound clinical judgment.

Conclusion

Within the limitation of this photoelastic study, implant diameter and ridge width had considerable influence on stress distribution. Narrow-diameter implants placed in both narrow and average ridge width models demonstrated higher stress to the model than standard- or wide-diameter implants placed in ridges with narrow and average buccolingual width. It is likely that the volume and quality of the bone surrounding implants influences stress distribution with a greater cortical to trabecular bone ratio providing better support. Wide-diameter implants demonstrated the least stress to the model as compared to narrow- and standard-diameter implants, with the least stress being distributed in the average ridge as compared to the narrow ridge.

Abbreviations

AR: average ridge
ND: narrow diameter
NR: narrow ridge
SD: standard diameter
WD: wide diameter

References

1. Albrektsson T, Zarb G, Worthington P, Eriksson AR. The long-term efficacy of currently used dental implants: a review and proposed criteria of success. *Int J Oral Maxillofac Implants*. 1986;1:11–25.

2. Shin YK, Han CH, Heo SJ, Kim S, Chun HJ. Radiographic evaluation of marginal bone levels around implants with different neck designs after 1 year. *Int J Oral & Maxillofac Implants*. 2006;20:789–794.

3. Georgiopoulos B, Kalioras K, Provatidis C, Manda M, Koidis P. The effects of implant length and diameter prior to and after osseointegration: a 2-D finite element analysis. *J Oral Implantol*. 2007;33:243–56.

4. Baggi L, Cappelloni I, Di Girolamo M, Maceri F, Vairo G. The influence of implant diameter and length on stress distribution of osseointegrated implants related to crestal bone geometry: a three-dimensional finite element analysis. *J Prosthet Dent*. 2008;100:422–431.

5. Graves SL, Jansen CE, Siddiqui AA, Beaty KD. Wide diameter implants: indications, considerations and preliminary results over a two-year period. *Aust Prosthodont J*. 1994;8:31–37.

6. Pellizzer EP, Verri FR, de Moraes SL, Falcón-Antenucci RM, de Carvalho PS, Noritomi PY. Influence of the implant diameter with different sizes of hexagon: analysis by 3-dimensional finite element method. *J Oral Implantol*. 2013;39:425–431.

7. Anitua E, Tapia R, Luzuriaga F, Orive G. Influence of implant length, diameter, and geometry on stress distribution: a finite element analysis. *Int J Periodontics Restorative Dent*. 2010;30:89–95.

8. Cordioli G, Majzoub Z. Heat generation during implant site preparation: an in vitro study. *Int J Oral Maxillofac Implants*. 1997;12:186–193.

9. Katranji A, Misch K, Wang H. Cortical bone thickness in dentate and edentulous human cadavers. *J of Periodontology*. 2007;78:874–878.

10. Proffit WR, Fields HW, Nixon WL. Occlusal forces in normal- and long-face adults. *J Dent Res*. 1983;62:566–570.

11. Sadowsky SJ, Caputo AA. Stress transfer of four mandibular implant overdenture cantilever designs. *J Prosthet Dent*. 2004;92:328–336.

12. Deguchi T, Nasu M, Murakami K, Yabuuchi T, Kamioka H, Takano-Yamamoto T. Quantitative evaluation of cortical bone thickness with computed tomographic scanning for orthodontic implants. *Am J Orthod Dentofacial Orthop*. 2006;129:721.

13. Akça K, Fanuscu M, Caputo A. Effect of compromised cortical bone in implant load distribution. *J Prosthodont*. 2008;17:616–620.

14. Farah JW, Craig RG, Sikarskie DL. Photoelastic and finite element stress analysis of a restored axisymmetric first molar. *J Biomech*. 1973;6:511–520.

15. Graves SL, Jansen CE, Siddiqui AA. Wide diameter implants: indications, considerations, and preliminary results over a two-year period. *Aust Prosthodont J*. 1994;8:31–37.

16. Gargallo Albiol J, Satorres-Nieto M, Puyuelo Capablo JL, Sánchez Garcés MA, Pi Urgell J, Gay Escoda C. Endosseous dental implant fractures: an analysis of 21 cases. *Med Oral Patol Oral Cir Bucal*. 2008;13:E124–E128.

17. Santiago Junior JF, Pellizzer EP, Verri FR, de Carvalho PS. Stress analysis in bone tissue around single implants with different diameters and veneering materials: a 3-D finite element study. *Mater Sci Eng C Mater Biol Appl*. 2013;33:4700–4714

18. Isidor, F. Loss of osseointegration caused by occlusal load of oral implants. *Clin Oral Impl Res*. 1996;7:143–152.

19. Conrad H, Schulte J, Vallee M. Fractures related to occlusal overload with single posterior implants: a clinical report. *J Prosthet Dent*. 2008;99:251–256.

20. Liaje A, Ozkan YK, Ozkan Y, Vanlioğlu B. Stability and marginal bone loss with three types of early loaded implants during the first year after loading. *Int J Oral Maxillofac Implants*. 2012;27:162–172.

21. Olate S, Lyrio MC, de Moraes M, Mazzonetto R, Moreira RW. Influence of diameter and length of implant on early dental implant failure. *J Oral Maxillofac Surg*. 2010;68:414–419.

22. Kim YK, Lee JH, Lee JY, Yi YJ. A randomized controlled clinical trial of two types of tapered implants on immediate loading in the posterior maxilla and mandible. *Int J Oral Maxillofac Implants*. 2013;28:1602–1611.

23. Pellizzer EP, Carli RI, Falcón-Antenucci RM, Verri FR, Goiato MC, Villa LM. Photoelastic analysis of stress distribution with different implant systems. *J Oral Implantol*. 2014;40:117–122.